Modulation of synaptic function through the α-neurexin–specific ligand neurexophilin-1

Gesche Born[a,1], Dorothee Breuer[a,1], Shaopeng Wang[a,1], Astrid Rohlmann[a], Philippe Coulon[b], Puja Vakili[a], Carsten Reissner[a], Friedemann Kiefer[c], Martin Heine[d], Hans-Christian Pape[b], and Markus Missler[a,2]

[a]Institute of Anatomy and Molecular Neurobiology, Westfälische Wilhelms-University, D-48149 Münster, Germany; [b]Institute of Physiology 1, Westfälische Wilhelms-University, D-48149 Münster, Germany; [c]Mammalian Cell Signalling Laboratory, Max Planck Institute for Molecular Biomedicine, D-48149 Münster, Germany; and [d]Molecular Physiology Group, Leibniz Institute of Neurobiology, D-39118 Magdeburg, Germany

Edited* by Thomas C. Südhof, Stanford University School of Medicine, Stanford, CA, and approved February 25, 2014 (received for review June 27, 2013)

Neurotransmission at different synapses is highly variable, and cell-adhesion molecules like α-neurexins (α-Nrxn) and their extracellular binding partners determine synapse function. Although α-Nrxn affect transmission at excitatory and inhibitory synapses, the contribution of neurexophilin-1 (Nxph1), an α-Nrxn ligand with restricted expression in subpopulations of inhibitory neurons, is unclear. To reveal its role, we investigated mice that either lack or overexpress Nxph1. We found that genetic deletion of Nxph1 impaired $GABA_B$ receptor ($GABA_BR$)-dependent short-term depression of inhibitory synapses in the nucleus reticularis thalami, a region where Nxph1 is normally expressed at high levels. To test the conclusion that Nxph1 supports presynaptic $GABA_BR$, we expressed Nxph1 ectopically at excitatory terminals in the neocortex, which normally do not contain this molecule but can be modulated by $GABA_BR$. We generated Nxph1-GFP transgenic mice under control of the Thy1.2 promoter and observed a reduced short-term facilitation at these excitatory synapses, representing an inverse phenotype to the knockout. Consistently, the diminished facilitation could be reversed by pharmacologically blocking $GABA_BR$ with CGP-55845. Moreover, a complete rescue was achieved by additional blocking of postsynaptic $GABA_AR$ with intracellular picrotoxin or gabazine, suggesting that Nxph1 is able to recruit or stabilize both presynaptic $GABA_BR$ and postsynaptic $GABA_AR$. In support, immunoelectron microscopy validated the localization of ectopic Nxph1 at the synaptic cleft of excitatory synapses in transgenic mice and revealed an enrichment of $GABA_AR$ and $GABA_BR$ subunits compared with wild-type animals. Thus, our data propose that Nxph1 plays an instructive role in synaptic short-term plasticity and the configuration with GABA receptors.

synaptic transmission | thalamus | autism | neuroligin | ultrastructure

Chemical synapses mediate signal transmission, integration, and plasticity. Synaptically transmitted signals differ between synapses of the same type and vary even at individual contacts of the same neuron (1), depending, for example, on their probability of release and history of activity (2, 3). Numerous studies have demonstrated that neurotransmission requires a plethora of synaptic molecules and signaling events (4). However, the mechanisms controlling the shaping of synapses with different properties are mostly unclear. We have addressed this problem by studying neurexins and their interaction partners (5, 6). Several aspects make neurexins candidates to couple local recognition/adhesion events to synaptic function: first, both extracellularly longer α-neurexins (α-Nrxn) and shorter β-neurexins (β-Nrxn) are able to induce functional synapses (7, 8); second, at least α-Nrxn are essential for synaptic transmission at excitatory and inhibitory terminals (9, 10); and third, α- and β-Nrxn are highly polymorphic, mostly presynaptic molecules (11, 12) that interact with *trans*-synaptic binding partners like neuroligins (13, 14), LRRTMs (15, 16), or cerebellin/GluRδ2 (17, 18).

In contrast to Nrxn that are expressed throughout the brain in virtually all excitatory and inhibitory neurons (12), the α-Nrxn–specific ligand neurexophilin (Nxph) is restricted to neuronal subpopulations (19, 20). The function of this ligand has not been studied in detail. Neurexophilins were discovered as a component of the latrotoxin receptor α-Nrxn (21) and comprise a family of four glycoproteins (Nxph1–4) that exhibit the characteristics of secreted, preproprotein-derived molecules (19, 22). Biochemical studies demonstrated that Nxph1 and Nxph3 interact with the second laminin-sex hormone-binding protein neurexin (LNS) domain of Nrxn (23). The LNS2 domain is present only in the extracellular sequences of α-Nrxn that contain six LNS domains, whereas β-Nrxn contain only a single LNS identical to the sixth domain of α-Nrxn (6).

In situ hybridization data suggested that Nxph1 is present in select inhibitory interneurons of the adult brain (19) and in migratory interneuron precursors (24). Knock-in mice coexpressing *lacZ* with Nxph3, in turn, revealed expression in excitatory neurons of neocortical layer 6b and in the vestibulocerebellum (20). The localized expression of Nxph variants is contrary to the widespread distribution of α-Nrxn, raising the question of whether Nxph have modulatory functions at distinct subpopulations of synapses. We observed previously that deletion of Nxph1 and Nxph3 in mice has no major impact on postnatal survival (20, 23), unlike their cognate receptor α-Nrxn (9), but no information on their physiological roles is available yet.

Here, we show that deletion of Nxph1 impairs $GABA_B$-receptor ($GABA_BR$)–dependent short-term depression of inhibitory synapses in the nucleus reticularis thalami (NRT). In support, transgenic overexpression of Nxph1 at excitatory contacts in the neocortex demonstrates the ability to alter the molecular composition of synapses because functional $GABA_A$ and $GABA_B$

Significance

Communication between neurons via synapses is essential for information processing and cognitive function in our brains and is found impaired in many neuropsychiatric disorders. Synaptic transmission is remarkably variable in strength, and cell-adhesion molecules as neurexins and their binding partners are candidates to regulate neurotransmission. This study changes our understanding of how neurotransmission can be adapted to local demands by investigating the previously undescribed functions of neurexophilins, arguably the most elusive ligands of α-neurexins. Neurexophilins are expressed only in subpopulations of synapses, and their presence is able to change short-term plasticity and molecular composition at these terminals.

Author contributions: G.B., S.W., A.R., M.H., H.-C.P., and M.M. designed research; G.B., D.B., S.W., A.R., P.V., C.R., and F.K. performed research; P.C., C.R., and F.K. contributed new reagents/analytic tools; G.B., D.B., S.W., A.R., P.C., C.R., M.H., H.-C.P., and M.M. analyzed data; and M.M. wrote the paper.

The authors declare no conflict of interest.

*This Direct Submission article had a prearranged editor.

Freely available online through the PNAS open access option.

[1]G.B., D.B., and S.W. contributed equally to this work.

[2]To whom correspondence should be addressed. E-mail: markus.missler@uni-muenster.de.

This article contains supporting information online at www.pnas.org/lookup/suppl/doi:10.1073/pnas.1312112111/-/DCSupplemental.

receptors become enriched and cause an impaired short-term facilitation.

Results

Nxph1 Functions at GABAergic Synapses in the Thalamus. To determine the physiological role of Nxph1 at synapses, we studied neurotransmission in Nxph1-deficient (KO) mice. We chose the NRT as a model system because expression of Nxph1 is normally high in the NRT (19). In addition, this region is composed of GABAergic neurons that sustain important brain functions, including sleep–wake regulation, cognition, and neuronal attention (25–27). Whole-cell patch-clamp recordings from Nxph1 KO neurons in the NRT (Fig. 1*A*) revealed only a small effect on spontaneous release because the frequency of miniature inhibitory postsynaptic currents (mIPSCs) was increased compared with wild type (WT) (Fig. 1 *B* and *C*). Amplitudes and kinetics such as decay times of mIPSCs were not different between genotypes (Fig. 1 *D* and *E*), and deletion of Nxph1 did not significantly alter electrically evoked inhibitory post synaptic currents (eIPSC amplitudes in WT: 418.5 ± 49.8 pA, $n = 19$ cells; in Nxph1 KO: 339.8 ± 54.1 pA, $n = 14$ cells; $P = 0.30$), although a tendency toward smaller responses in KO may exist. To test the hypothesis that Nxph1 might affect synaptic plasticity more strongly than basic transmission, we performed paired-pulse experiments to evoke short-term plasticity in the NRT (Fig. 1*F*). Short-term depression of eIPSCs, typical for NRT synapses (28), was impaired in KO neurons and replaced by facilitation at short interstimulus intervals, indicating that short-term depression as analyzed by paired-pulse ratio (ppr) depends on Nxph1 (Fig. 1*G*). This finding is supported by a second experimental protocol, a 20-Hz stimulation pulse that also yielded strong depression in NRT neurons of WT but not of KO mice (Fig. 1 *H1*, *H2*, and *I*), providing further evidence for a role of Nxph1 in synaptic plasticity. In contrast, basal neuronal cell properties such as membrane input resistance, resting potential, and capacitance were equal in both genotypes (Table S1). Current-clamp recordings of low-threshold spikes (LTS), a characteristic rebound response of NRT neurons (29, 30), also remained unchanged in the absence of Nxph1 (Fig. 1*J* and Table S1), suggesting that Nxph1 is not required for mediating intrinsic properties of the GABAergic NRT neurons.

Because paired-pulse depression and spontaneous release at inhibitory terminals of NRT involves activation of $GABA_BR$ (31), we probed the possibility that Nxph1 affects the function of these receptors by applying the antagonist CGP-55845 (Fig. 2*A*). We observed that mIPSC frequencies in KO were only weakly affected by (2S)-3-[[(1S)-1-(3,4-Dichlorophenyl)ethyl]amino-2-hydroxypropyl](phenylmethyl)phosphinic acid hydrochloride

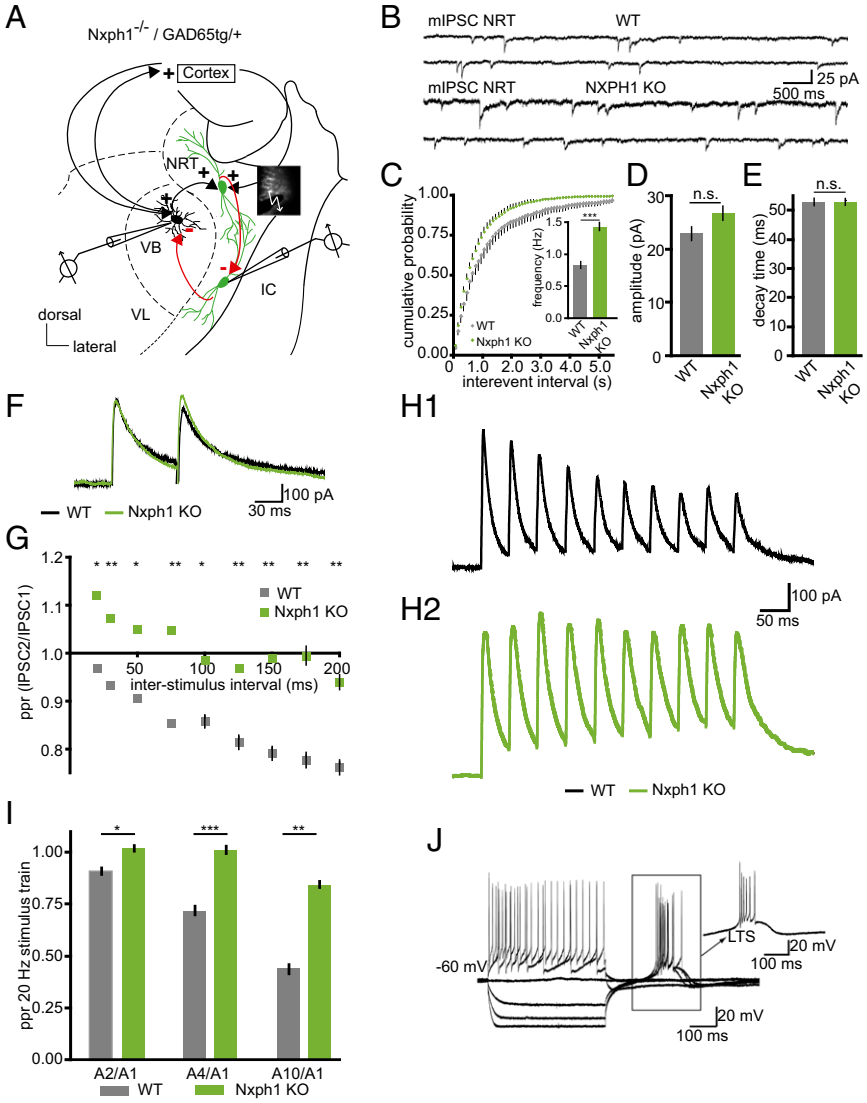

Fig. 1. Nxph1 functions in subpopulations of inhibitory synapses. (*A*) Experimental setup for patch-clamp recordings from neurons in the NRT (green indicates GAD65-driven GFP for reliable identification) and the VB. IC, internal capsule; VL, ventral posterolateral nucleus. Red arrows indicate GABAergic connections analyzed within the NRT and to the VB. (*B*) Representative mIPSC recordings from NRT neurons of WT (*Upper* traces) and Nxph1 KO (*Lower* traces). (*C–E*) mIPSC frequencies in KO neurons (green) show a leftward shift in the cumulative representation, and an increased average (*Inset*). Amplitudes (*D*) and decay times (*E*) of mIPSC are similar in both genotypes. (*F*) Averaged current traces from paired-pulse experiments in WT (black) and KO (green) to evoke inhibitory synaptic short-term depression. (*G*) Paired-pulse depression seen in WT at different interstimulus intervals is abolished in KO. (*H* and *I*) Short-term plasticity in NRT neurons evoked by a 20-Hz stimulus train (H_1, sample traces from WT; H_2, sample traces from KO) reveals depression in WT. Ratios (ppr) were calculated between the 2nd, 4th, and 10th amplitude to the first amplitude, but depression (<1.0) was hardly observed in KO (*I*). (*J*) Representative current-clamp recording from KO showing LTS after hyperpolarization (arrow). All data are means ± SEM (collected from 10 to 19 neurons from at least three mice per condition/genotype). Significance of differences was tested by Student *t* test for unpaired values; levels are indicated as $*P < 0.05$, $**P < 0.01$, and $***P < 0.001$. n.s., not significant.

(CGP), whereas in WT, they were increased to the level of Nxph1-deficient neurons (Fig. 2*B*). Amplitudes and decay times of mIPSCs were not changed by CGP treatment in either of the two genotypes (Fig. 2 *C* and *D*), consistent with a lack of phenotype in these control parameters (Fig. 1 *D* and *E*). More importantly, paired-pulse depression of inhibitory synapses in WT was reduced upon CGP application (Fig. 2*E*), approaching values for KO neurons, whereas the paired-pulse ratio in KO remained largely unchanged (Fig. 2*F*). These data show that deletion of Nxph1 produced a phenotype that behaves as if the activity of $GABA_BRs$ is blocked. Our results are consistent with earlier reports demonstrating that blockade of $GABA_BR$ at inhibitory synapses in NRT cells and elsewhere reverses paired-pulse depression (31, 32) and that presynaptic $GABA_BR$ at inhibitory terminals are involved in the sustained depression of GABA-mediated transmission (32–34). Although clearly not all inhibitory synapses in the brain contain $GABA_B$ autoreceptors (35), addition of the $GABA_BR$ agonist baclofen in some experiments also confirmed that wild-type NRT neurons are regulated by these autoreceptors (31) and that Nxph1-deficient cells respond less to application of the agonist (Fig. S1). Thus, our analysis demonstrates that deletion of Nxph1 impairs $GABA_BR$-mediated inhibition at GABAergic synapses in the NRT and that Nxph1 is required for short-term plasticity at these terminals.

Because Nxph were initially characterized as putatively secreted, neuropeptide-like molecules based on sequence analysis (22), a diffuse, paracrine mode of action could not be excluded. To test if the role of Nxph1 was restricted to brain regions with abundant expression such as the NRT, we performed control recordings of pharmacologically isolated GABAergic synapses in layer 5 of the somatosensory cortex (Fig. 3 *A* and *B*), a region with very low expression of Nxph1 in WT (19). Quantitative analysis revealed no significant differences between WT and KO neurons in mIPSC frequency (Fig. 3*C*), amplitude (Fig. 3*D*), decay time (Fig. 3*E*), and ppr (Fig. 3*F*). These results support the conclusion that the observed effects are restricted to regions of significant Nxph1 expression.

To probe if the impairments were restricted to intrinsic NRT synapses or present at other terminals of NRT neurons, we performed additional recordings from neurons of the thalamic ventrobasal nucleus (VB) that receive GABAergic projections from NRT neurons (Fig. 1*A*). In contrast to NRT, quantitative RT-PCR (qRT-pCR) experiments showed that VB neurons in mice express very little Nxph1 mRNA themselves (VB: 0.57 ± 0.03; NRT: 5.09 ± 0.53; $n = 3$, $P = 0.0066$), in particular compared with α-Nrxn that show an equal distribution (Nrxn3α in VB: 2.47 ± 0.43; NRT: 2.28 ± 0.59; $n = 3$, $P = 0.84$). In line with this finding, recordings of spontaneous release (Fig. 3*G*) and short-term depression (Fig. 3*H*) failed to detect any changes in the VB of Nxph1 KO animals, supported by quantification of mIPSC frequency (Fig. 3*I*), amplitude (Fig. 3*J*), decay time (Fig. 3*K*), and ppr (Fig. 3*L*). Thus, our results propose that deletion of Nxph1 causes a remarkably specific impairment of intrinsic GABAergic NRT synapses that is undetectable at the VB projection from the same neurons or at inhibitory synapses in brain regions with only low endogenous Nxph1 expression.

Expression of Nxph1 Has an Instructive Role in Synapses. Based on our analysis of KO mice, we hypothesized that expression of Nxph1 at synapses is highly regulated and may stabilize metabotropic $GABA_BR$. To test this idea, we introduced Nxph1 ectopically as a fusion protein with EGFP in transgenic mice (Nxph1-$GFP^{tg/-}$, Fig. 4*A*). Nxph1-GFP was expressed under control of the Thy1.2 promoter, for example, in a large population of pyramidal neurons in the neocortex of transgenic mice (Fig. 4*B*; and Fig. 4*C* as WT control), indicating that Nxph1-GFP was present in excitatory neurons, which normally do *not* contain this α-Nrxn ligand (19). This strategy was conceived to artificially drive Nxph1 into synapses that usually lack this molecule, allowing us to compare normal physiological properties to the effects of introducing Nxph1.

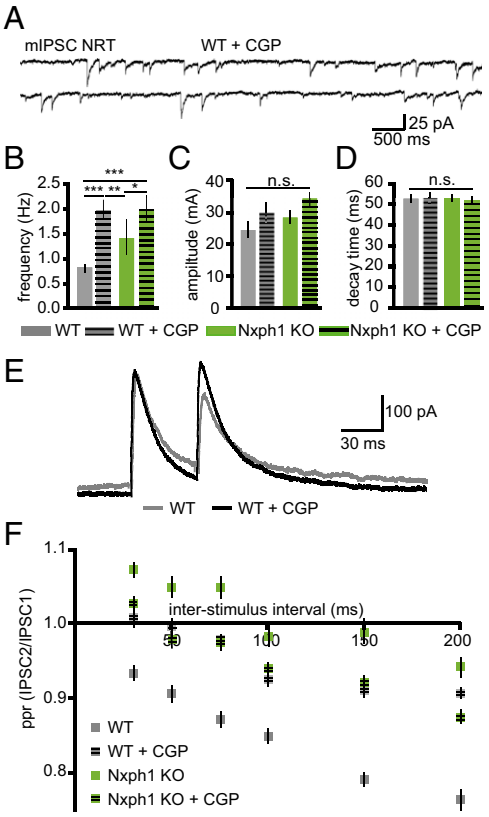

Fig. 2. Blockade of $GABA_BR$ in the NRT mimics the effect of Nxph1 deletion. (*A*) mIPSC recordings from WT neurons in the NRT with the $GABA_BR$ inhibitor CGP-55845. (*B–D*) mIPSC frequencies are increased in the presence of CGP in WT, whereas KO frequencies remain elevated (*B*). Amplitudes (*C*) and decay times (*D*) are unaffected by $GABA_BR$ blockade. (*E*) Averaged current traces of paired-pulse experiments in WT neurons of the NRT without (gray) and with CGP (black). (*F*) Depression normally seen in NRT neurons at different interstimulus intervals can be blocked by CGP. No significant changes occur after blockade in KO neurons. All data are means ± SEM (collected from 8 to 19 neurons from at least three mice per condition/genotype). Significance of differences was tested for several combinations of datasets as shown by horizontal lines in *B* (WT vs. WT+CGP, KO vs. KO vs. KO+CGP, etc.) using Student *t* test for unpaired values (the same combinations were tested in *C* and *D*, but no differences were found). Levels are indicated as $*P < 0.05$, $**P < 0.01$, $***P < 0.001$. n.s., not significant.

As prerequisite for functional experiments, we first investigated if Nxph1-GFP was actually localized at excitatory synapses of transgenic mice. Immunoelectron microscopy was performed with anti-GFP antibodies in the neocortex of WT and transgenic animals. We found almost 10-fold more labeling with 10 nm gold particles at asymmetric type 1 (putative excitatory) synapses in mutants compared with low background levels in WT samples (WT: 0.40 ± 0.23/1,000 μm^2; Nxph1-$GFP^{tg/-}$: 3.66 ± 0.70/1,000 μm^2; $n = 4$; $P = 0.004$). To safeguard against artifacts, three methods were applied, which all revealed labeled excitatory synapses in Nxph1-$GFP^{tg/-}$ mice (Fig. 4 *D–F*). Nxph1-GFP was frequently located directly over synaptic clefts (Fig. 4 *D–F*) at the plasma membrane of presynaptic terminals (Fig. 4*G*) and at extrasynaptic sites of the cell surface (Fig. 4*H*), consistent with the mobile behavior of its cognate receptor α-Nrxn on axonal membranes (36). Intracellularly, we observed gold-labeled Nxph1 over vesicular structures in the presynaptic terminal (Fig. 4*I*) and inside the lumen of rough endoplasmatic reticulum (rER) and Golgi cisternae (Fig. 4 *J* and *K*), as expected for a glycoprotein that traverses the secretory pathway (22). To assess if overexpression of Nxph1 had an effect on synaptic architecture in general, we studied synapse distribution and ultrastructure in

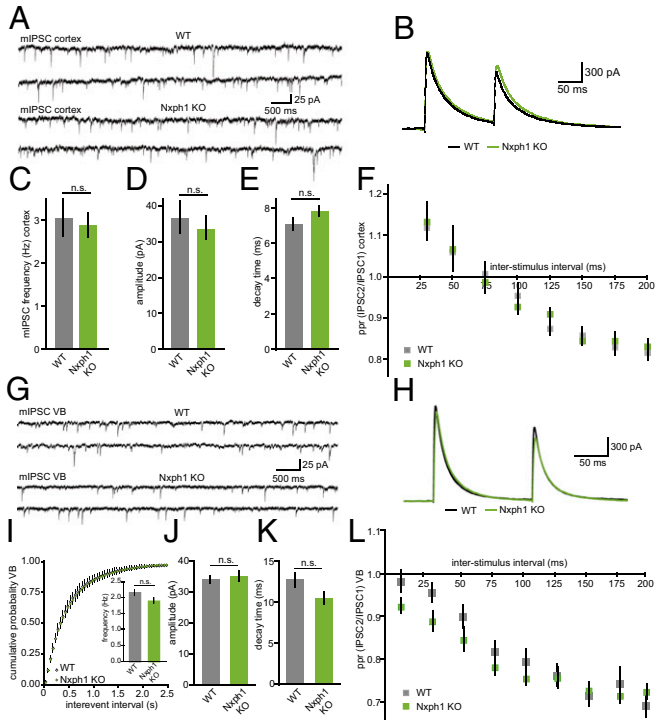

Fig. 3. Low-expressing interneurons are unaffected in Nxph1 KO. (*A*) Pharmacologically isolated mIPSCs recorded from neocortical layer 5 neurons of WT (*Upper* traces) and KO (*Lower* traces). (*B*) Paired-pulse experiments in these neurons show similar depressing characteristics (gray, WT; green, Nxph1 KO). (*C–E*) In contrast to NRT (Fig. 1), mIPSC frequencies in the neocortex are unchanged between genotypes (*C*), as are amplitudes (*D*) and decay time constants (*E*). (*F*) Quantification of ppr from experiments shown in *B* reveal normal inhibitory short-term plasticity in Nxph1 KO. Similar recordings of mIPSCs (*G*) and ppr (*H*) in the VB of the thalamus also fail to detect differences in mini parameters (*I–K*) and synaptic depression (*L*). All data are means ± SEM (collected from 8 to 19 neurons from at least three mice per condition/genotype). Significance of differences was tested by Student *t* test for unpaired values. n.s., not significant.

Nxph1-GFP$^{tg/-}$ and WT. The numbers of asymmetric synapses (type 1; WT: 22.62 ± 0.86/100 μm^2; Nxph1-GFP$^{tg/-}$: 22.75 ± 1.29/100 μm^2; $P = 0.93$) and symmetric synapses (type 2; WT: 3.15 ± 0.15/100 μm^2; Nxph1-GFP$^{tg/-}$: 3.62 ± 0.41/100 μm^2; $P = 0.31$) remained unchanged. Similarly, terminal area (WT: 0.197 ± 0.0164 μm^2; Nxph1-GFP$^{tg/-}$: 0.194 ± 0.0214 μm^2; $P = 0.73$), vesicle density (WT: 203 ± 11/μm^2, Nxph1-GFP$^{tg/-}$: 211 ± 19/μm^2; $P = 0.46$), length of postsynaptic density (WT: 287.6 ± 9.22 nm; Nxph1-GFP$^{tg/-}$: 293.6 ± 7.19 nm; $P = 0.31$), or width of synaptic cleft (WT: 22.62 ± 0.95 nm; Nxph1-GFP$^{tg/-}$: 21.69 ± 1.15 nm; $P = 0.48$) were also not impaired. These results indicate that overexpression of Nxph1 has no major impact on synapse morphology, but the localization within the synaptic cleft is in accordance with a role in short-term plasticity as predicted from our KO analysis above.

To study the functional consequences of ectopic Nxph1 at excitatory synapses, we performed whole-cell patch-clamp recordings from layer 5 pyramidal neurons of the primary somatosensory cortex. Evoked responses in this region were elicited by a stimulation electrode placed in layer 5 about 100 μm laterally of the recorded neurons. No differences between Nxph1-GFP$^{tg/-}$ and WT were observed for parameters of membrane properties and for spontaneous release of miniature excitatory postsynaptic currents (mEPSCs) (Fig. 5 *A–D*) and inhibitory mini release (mIPSCs) (Fig. 5 *E–H*). However, probing short-term plasticity with paired-pulse experiments at excitatory synapses that express Nxph1 revealed a striking alteration in ppr. Facilitation could be elicited in WT synapses over a wide range of interstimulus intervals (20–150 ms) but was significantly diminished in Nxph1-GFP$^{tg/-}$ mice (Fig. 6*A*). The impairment even showed depressing characteristics at longer intervals and was independent of stimulus intensities (Fig. 6*B*). As an additional control, we tested short-term plasticity at inhibitory synapses but failed to detect differences (Fig. 6 *C* and *D*), consistent with our EM data that detected Nxph1-GFP only at excitatory terminals (Fig. 4 *D–F*). Importantly, changes in basal transmission or cellular excitability were not responsible for the alterations of short-term plasticity because amplitudes elicited by single electrical stimulation evoked EPSC ($eEPSC_{halfmax}$ in WT: −1,327 ± 97 pA, $n = 20$ cells; in Nxph1-GFP$^{tg/-}$: −1,320 ± 107 pA, $n = 21$ cells; $P = 0.96$) and time constants of these eEPSCs were indistinguishable (decay $time_{halfmax}$ in WT: 24 ± 1.7 ms, $n = 20$ cells; in Nxph1-GFP$^{tg/-}$: 25 ± 1.7, $n = 21$ cells/genotype, $P = 0.68$).

Because the impairment of paired-pulse facilitation at transgenic synapses represents an inverse effect compared with KO neurons (Fig. 1*G*), we asked if overexpression of Nxph1 affected $GABA_BR$ activity, as did its deletion (Fig. 2). We probed this by adding the $GABA_BR$ antagonist CGP-55845 during paired-pulse experiments (Fig. 7*A*). Impaired facilitation of evoked postsynaptic currents at excitatory synapses with Nxph1 could partially be rescued by the CGP treatment (Fig. 7 *A* and *B*), even if ppr values did not fully reach WT levels at all interstimulus intervals (Fig. 7*B*). In contrast, excitatory short-term plasticity of WT neurons showed almost no significant differences during action of CGP (Fig. 7*B*, e.g., at 50 and 100 ms). To test if CGP influenced the size of eEPSCs in transgenic neurons, we analyzed responses at low-stimulus intensities to avoid summation effects from large inward currents that would obscure monosynaptic PSCs. Amplitudes from both genotypes were comparable and independent of treatment (WT + CGP: −461 ± 24 pA, $n = 22$ cells/five mice; Nxph1-GFP$^{tg/-}$ + CGP: −484 ± 46 pA, $n = 17$ cells/five mice; $P = 0.64$), consistent with an intact basal transmission at synapses with or without ectopic Nxph1. Although these results from transgenic overexpression are in agreement with our lack-of-function data by indicating that functional $GABA_BR$ are one putative target of Nxph1, at present we cannot say whether this link involves direct interactions. However, because the impaired facilitation in Nxph1-GFP$^{tg/-}$ could not be fully rescued to WT levels by CGP application (Fig. 7*B*), we suspected that additional target molecules might be involved in the process.

In fact, previous work already pointed to another putative target, i.e., the ionotropic $GABA_AR$ family because the Nxph1-binding partner α-Nrxn has been reported to cluster $GABA_AR\gamma2$ subunits (7) and directly associates with $GABA_AR\alpha1$ (37). Therefore, we tested if $GABA_AR$ also contributes to the altered short-term plasticity of transgenic synapses by blocking $GABA_AR$ with intracellular application of picrotoxin or gabazine (Fig. 7 *C–E*) and bath application of bicuculline (Fig. 7*E*) to distinguish between pre- and postsynaptic $GABA_AR$ populations (38). To ensure that postsynaptic $GABA_AR$ can be truely inhibited by intracellular application of picrotoxin or gabazine from the approaching pipette, we performed two control experiments: (*i*) In two-step tip-filling experiments (39), the recording pipette was first prefilled up to 500 μm with normal pipette solution without blocker and then backfilled with internal solution containing inhibitors (Fig. 7*C*). After establishment of whole-cell configuration, eIPSCs were recorded from layer 5 WT neurons, revealing that amplitudes of eIPSCs decreased in a time-dependent manner as expected for gradual diffusion of picrotoxin or gabazine from the pipette (Fig. 7*C* and Fig. S2). (*ii*) We compared the ppr at WT and Nxph1-GFP$^{tg/-}$ synapses 1 and 10 min after obtaining the whole-cell configuration (40) but observed no differences due to the washout between time points (ppr WT_1: 1.13 ± 0.05, $n = 16$ cells/three mice; WT_{10}: 1.15 ± 0.08, $n = 16$ cells/three mice, $P = 0.86$; Nxph1-GFP_1: 1.17 ± 0.08, $n = 14$ cells/three mice; Nxph1-GFP_{10}: 1.19 ± 0.06, $n = 16$ cells/three mice, $P = 0.83$).

Importantly, during intracellular blockade of $GABA_AR$ with 200 μM picrotoxin (Fig. 7 *D* and *E*) or 50 μM gabazine (Fig. 7*E*)

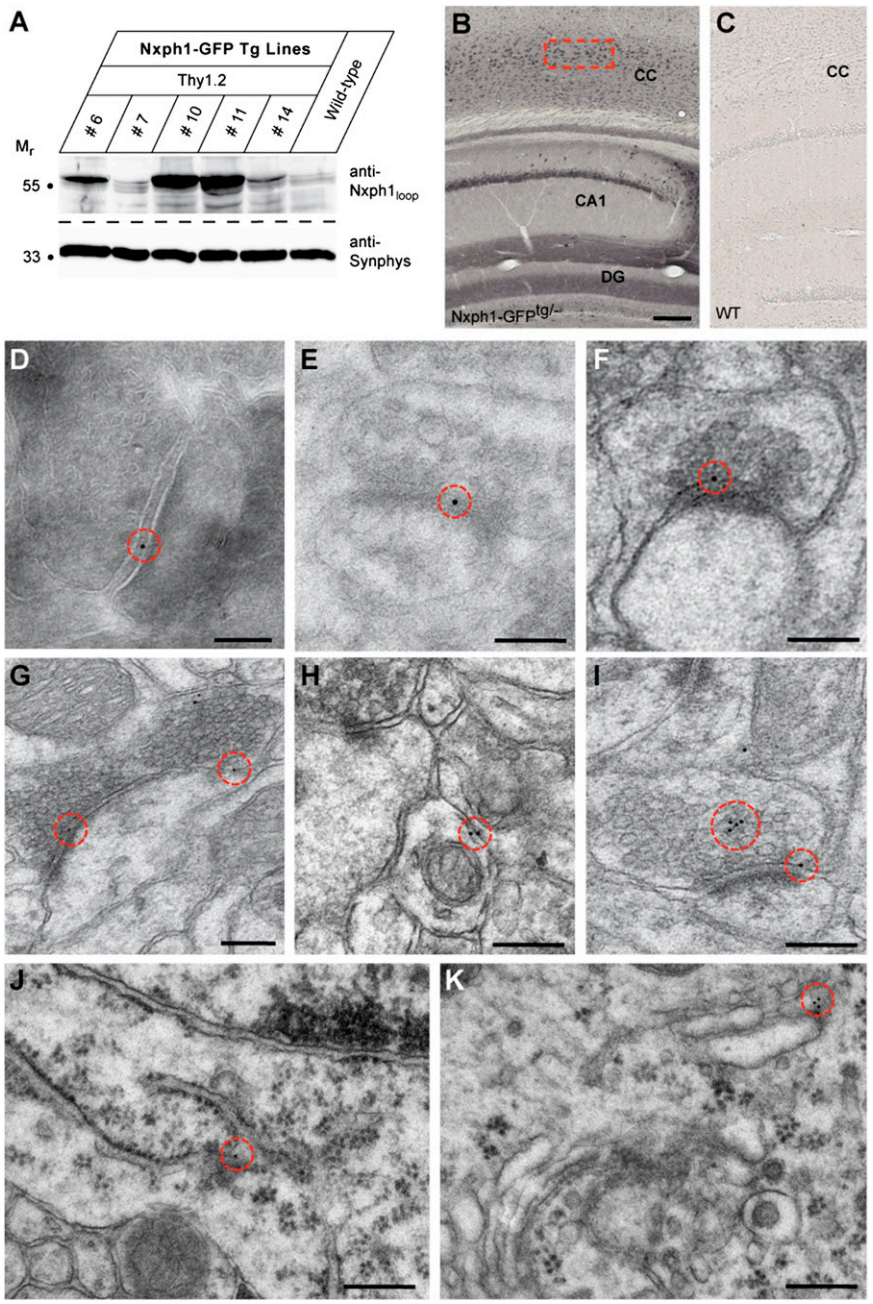

Fig. 4. Ectopic expression of Nxph1 at excitatory synapses. (*A*) Several Nxph1-GFP$^{tg/+}$ transgenic mouse lines express the fusion protein as evidenced by immunoblots of brain lysates. (*B* and *C*) Light microscopic images of immunohistochemistry with anti-GFP antibodies show Nxph1-GFP in brain sections of transgenic animals (*B*, line #10 from *A*). WT sections are devoid of any staining (*C*). CC, cerebral cortex; CA1 region, hippocampus; DG, dentate gyrus. (Scale bar, 150 μm.) (*D–F*) Different methods of EM immunolabeling were applied to localize Nxph1-GFP in the somatosensory cortex of transgenic brains (boxed area in *B*). Tokuyasu cryosectioning (*D*), Lowicryl postembedding (*E*), and Epon postembedding (*F*) techniques show 10-nm gold particles (circled in red) at synaptic clefts of asymmetric (presumptive excitatory) contacts. (Scale bars, 100 nm.) (*G–K*) In addition to the synaptic cleft, immunolabeling was found at the presynaptic plasma membrane outside active zones (*G*), at extrasynaptic sites of the cell surface (*H*), (*I*) intracellularly over vesicular structures in the terminal, and inside the lumen of rER (*J*) and Golgi cisternae (*K*). (Scale bars, 200 nm.)

in the recording pipette, paired-pulse facilitation at excitatory synapses of Nxph1-GFP$^{tg/-}$ neurons was indistinguishable from WT controls (Fig. 7*E*). These results imply that postsynaptic $GABA_AR$ populations contribute to the Nxph1-GFP$^{tg/-}$ phenotype. Consistently, the same results were obtained upon inclusion of 2 μM bicuculline in bathing medium (Fig. 7*E*) that inhibits both pre- and postsynaptic $GABA_AR$ populations. As control, extra- or intracellular addition of antagonists had almost no effects on ppr in WT neurons (Fig. 7*F*).

To test if the combined effects of $GABA_AR$ and $GABA_BR$ are sufficient to fully explain the impaired short-term plasticity, we finally used the concomitant application of bicuculline and CGP in bath solution (Fig. 7*G*). We observed that a simultaneous blockade of both $GABA_AR$ and $GABA_BR$ reversed the ppr impairments of transgenic synapses completely (Fig. 7*H*), reaching values very similar to WT. In contrast, the combined application of CGP and bicuculline had no influence on amplitudes of eEPSCs of both genotypes at low-stimulus intensities (WT + CGP + bicuculline: −160 ± 20 pA, n = 20 cells/six mice; Nxph1-GFP$^{tg/-}$ + CGP + bicuculline: −140 ± 15 pA, n = 25 cells/six mice; P = 0.43), indicating that GABARs specifically influenced short-term plasticity.

In absence of any indications for polysynaptic mechanisms that could explain the unexpected role of GABAR in our paired-pulse experiments, it is possible that $GABA_BR$ and $GABA_AR$ subunits become enriched in excitatory synapses of Nxph1-GFP$^{tg/-}$ neurons. To test if typical subunits of $GABA_AR$ and $GABA_BR$ were present at these terminals, we first used antibodies against the $GABA_AR\alpha1$ subunit for immunoelectron microscopy in transgenic mice because it should give a low endogenous background at excitatory synapses and is widely distributed at inhibitory terminals (41). In addition to expected labeling of symmetric (inhibitory) terminals in the neocortex of WT and Nxph1-GFP$^{tg/-}$ mice, we found numerous asymmetric, presumably excitatory, synapses in transgenic samples that

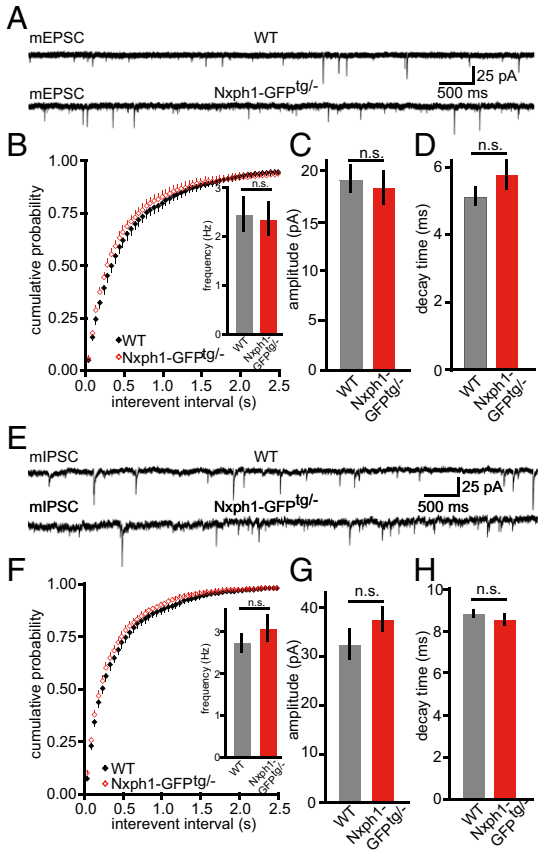

Fig. 5. Transgenic expression of Nxph1 has no effect on basal synaptic transmission. (*A*) Sample traces of glutamatergic mEPSCs recorded from cortical layer 5 neurons of WT (*Upper* trace) and Nxph1-GFP$^{tg/-}$ (*Lower* trace) mice. (*B*) Cumulative distribution and averaged (*Inset*) frequency of mEPSCs is not altered at transgenic synapses (WT, gray; Nxph1-GFP$^{tg/-}$, red). Similarly, peak amplitudes (*C*) and decay time constants (*D*) were not different. Data are means ± SEM (collected from 17 WT cells from eight animals and 10 cells from seven mice of Nxph1-GFP$^{tg/-}$). n.s., not significant. (*E*) Sample traces of inhibitory minis (mIPSCs). (*F*) Cumulative frequency and average (*Inset*) of mIPSCs is not altered at Nxph1-GFP$^{tg/-}$ synapses, which is similar to amplitudes (*G*) and decay time constants (*H*) of mIPSCs. Data are means ± SEM (collected from 19 WT cells from 6 mice and 34 Nxph1-GFP$^{tg/-}$ cells from 11 mice). n.s., not significant.

displayed 10 nm gold particles over the synaptic cleft (Fig. 8 *A* and *B*). Quantification of gold particles revealed a larger number of $GABA_AR\alpha1$-positive asymmetric synapses in transgenic mice (WT: 4.7 ± 0.03/1,000 μm^2, n = 4 mice; Nxph1-GFP$^{tg/-}$: 10.4 ± 1.01/1,000 μm^2, n = 4 mice; P = 0.011), indicating that ectopic expression of Nxph1 led to enrichment of receptor subunits. The few immunolabeled asymmetric profiles detected in WT (Fig. 8*C*) may reflect colocalization of $GABA_AR$ at glutamatergic synapses reported before (41). As the experiments with intracellular application of picrotoxin and gabazine suggested that $GABA_AR$ are enriched postsynaptically in transgenic synapses (Fig. 7*E*), we could probe if they are more likely recruited from extrasynaptic surface populations or inserted de novo from intracellular pools. We locally applied GABA via a puff pipette (10 mM) to layer 5 pyramidal neurons and recorded $GABA_AR$-dependent PSCs. No difference was found between WT and Nxph1-GFP$^{tg/-}$ without (GABA-evoked amplitudes in WT: 1,197 ± 155 pA, n = 11 cells/five mice; in Nxph1-GFP$^{tg/-}$: 1,162 ± 122 pA, n = 14 cells/five mice; P = 0.86) or with an additional block of $GABA_BR$ by CGP (WT_{CGP}: 1,080 ± 164 pA, n = 11 cells/five mice; in Nxph1-GFP$^{tg/-}{}_{CGP}$: 1,107 ± 125 pA, n = 14 cells/five mice; P = 0.89). These results suggest that the total surface density of $GABA_AR$ is similar, but a shift from the extrasynaptic population to transgenic synapses may occur if Nxph1 is present.

Because electrophysiological analysis of transgenic excitatory synapses also suggested enhanced presence of $GABA_BR$ (Fig. 7), we tested if they were also enriched by ectopic expression of Nxph1. Although WT terminals in the neocortex contain functional $GABA_BR$ (42, 43), we observed a significantly increased number of $GABA_BR1$-positive asymmetric synapses in transgenic mice (WT: 6.3 ± 0.83/1,000 μm^2, n = 3 mice; Nxph1-GFP$^{tg/-}$: 31.1 ± 3.11/1,000 μm^2, n = 3 mice; P = 0.013). Such an enrichment is consistent with the pharmacological rescue of the transgenic phenotype by addition of CGP (Fig. 7) and the finding of impaired $GABA_BR$-dependent plasticity in NRT synapses of knockout animals (Figs. 1–2). Together, these data demonstrate that expression of Nxph1 at synapses that normally do not contain this molecule is able to change their physiological properties and molecular composition.

Discussion

Neurotransmission at most synapses requires the synaptic cell adhesion molecules, α-Nrxn (9, 10, 37, 44–47). However, the ability of synapses to undergo synaptic plasticity (48, 49) and the local coordination of these rearrangements (50) indicate that α-Nrxn–mediated functions should be locally modulated. Here, we propose that the α-Nrxn–specific binding partner Nxph1 subserves such a modulatory role in subpopulations of synapses.

Physiological Role of Nxph1. Two independent experimental strategies support our conclusion because both deletion of Nxph1 in KO and ectopic overexpression of Nxph1-GFP in transgenic mice demonstrate a role of this α-Nrxn ligand in synaptic short-term plasticity. The conclusion is based on the following considerations (a graphical summary is provided in Fig. S3): Analysis of Nxph1-deficient inhibitory terminals reveals decreased paired-pulse depression at inhibitory synapses in the NRT (Fig. 1 and

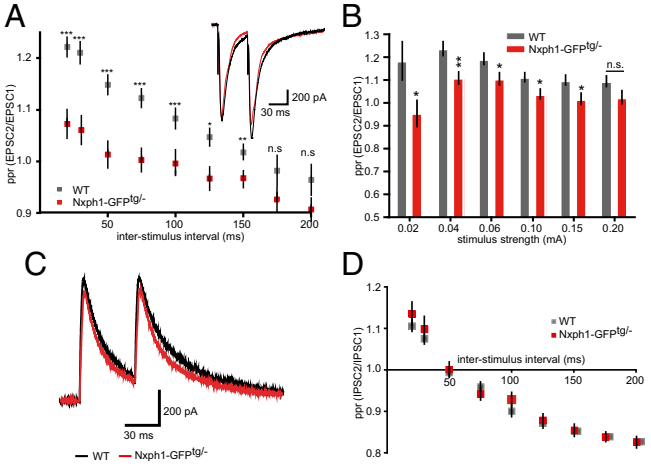

Fig. 6. Presence of Nxph1 impairs synaptic short-term plasticity at excitatory terminals. (*A*) Current traces from paired-pulse experiments and analysis of their ratios (ppr) at different interstimulus intervals in excitatory cortical synapses of WT (gray) and Nxph1-GFP$^{tg/-}$ (red). Note the reduced facilitation in transgenic mice. (*B*) Facilitation of excitatory Nxph1-GFP$^{tg/-}$ synapses is impaired at interstimulus intervals of 50 ms over a wide range of stimulus strengths. Data are means ± SEM (collected from 7 to 25 neurons from at least seven to eight mice per condition/genotype). Significance of differences was tested by Student *t* test for unpaired values; levels are indicated as $*P < 0.05$, $**P < 0.01$, and $***P < 0.001$. n.s., not significant. (*C*) Representative traces of paired-pulse experiments from inhibitory synapses at 50-ms interstimulus intervals. (*D*) Calculation of corresponding ppr values reveals depression with increasing interstimulus intervals but no differences between genotypes. (*C* and *D*) Data are means ± SEM (collected from 11 WT cells from three mice and 19 Nxph1-GFP$^{tg/-}$ cells from seven mice).

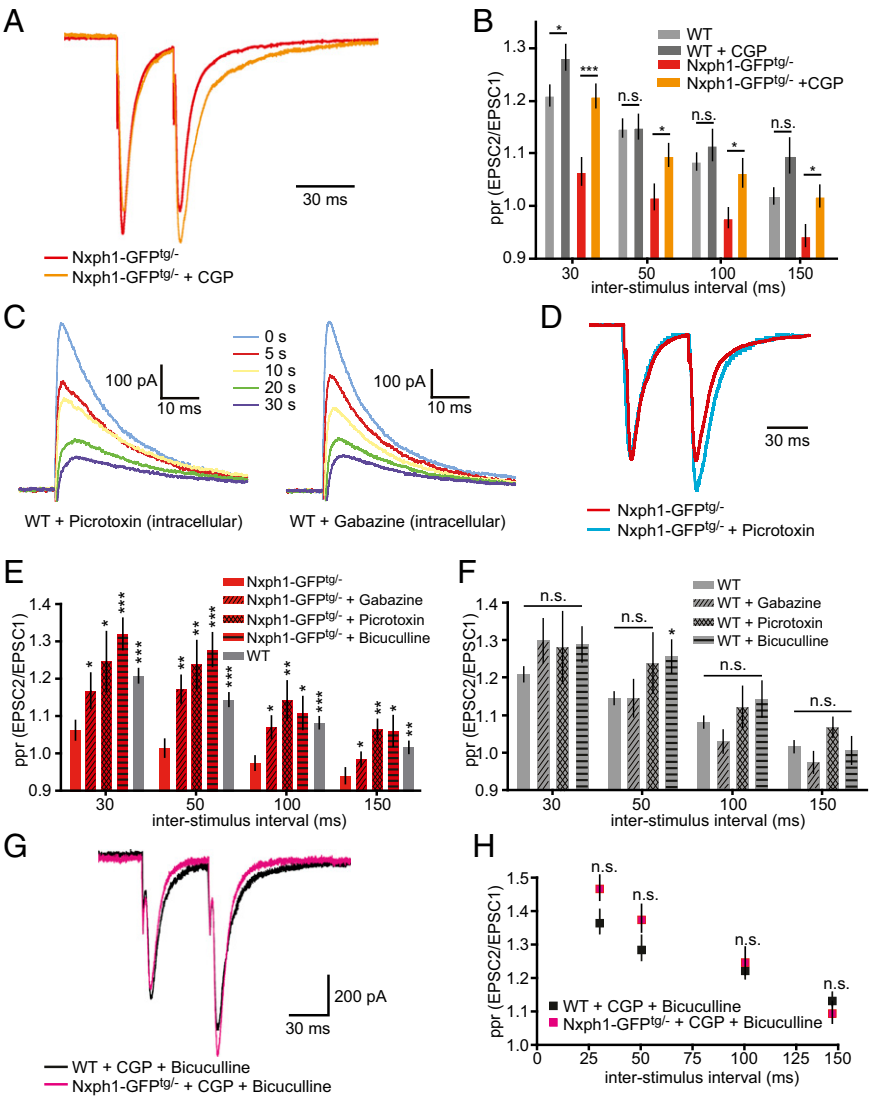

Fig. 7. The effect of Nxph1 on short-term plasticity depends on functional $GABA_A$ and $GABA_B$ receptors. (*A*) Normalized amplitude traces of paired-pulse experiments from Nxph1-$GFP^{tg/-}$ neurons (red) change after CGP treatment toward facilitation (orange). (*B*) Analysis of different interstimulus intervals demonstrates that reduced ppr in Nxph1-$GFP^{tg/-}$ is partially rescued by the $GABA_BR$ inhibitor (orange), whereas facilitation in WT neurons (light gray) remains almost unchanged (dark gray). (*C*) Averaged current traces of eIPSCs activated by single electrical pulses at 0.20 mA from WT neurons and recorded at indicated times after obtaining the whole-cell configuration. Patch pipettes were tip-filled with internal solution free of blockers and backfilled with solution containing either picrotoxin or gabazin. Recorded eIPSCs decreased in amplitude in a time-dependent manner, indicating gradual diffusion of gabazine or picrotoxin into the cell (time of first amplitude reduction defined as 0 s; for picrotoxin, $n = 7$ cells/four mice; for gabazine, $n = 8$ cells/three mice). (*D*) Normalized amplitude traces of paired-pulse experiments from Nxph1-$GFP^{tg/-}$ neurons without (red) and with intracellular application of picrotoxin (blue). (*E*) Treatment of Nxph1-$GFP^{tg/-}$ (red) with $GABA_AR$ inhibitors bicuculline (bath application), picrotoxin, or gabazine (intracellular application) restores ppr to WT levels (gray). (*F*) Treatment of WT with bicuculline, picrotoxin, or gabazine has almost no effect on ppr. (*G*) Current traces of ppr experiments during combined treatment with CGP and bicuculline to block $GABA_B$ and $GABA_A$ receptors (WT, black; Nxph1-$GFP^{tg/-}$ magenta). (*H*) Facilitation during simultaneous application at different interstimulus intervals shows that normal ppr levels are restored in Nxph1-$GFP^{tg/-}$. Data are means ± SEM (collected from 7 to 25 neurons from seven to eight mice per condition/genotype). Significance of differences was tested for several combinations of datasets as shown by horizontal lines in *B* (in *E* and *F*, comparisons are against the values of the first bar) using Student *t* test for unpaired values. Levels are indicated as $*P < 0.05$, $**P < 0.01$, and $***P < 0.001$. n.s., not significant.

Fig. S3*A*), and this KO phenotype can be mimicked by blocking presumably presynaptic $GABA_BR$ in WT neurons (Fig. 2) (31). An additional effect of Nxph1 on the $GABA_BR$-mediated inhibitory potential, required for synchronized burst firing of NRT neurons (28), is unlikely because unchanged eIPSCs and LTS generation argue against a strong influence on the postsynaptic population. Control recordings of GABAergic terminals in neocortex and the thalamic VB nucleus do not show alterations (Fig. 3), indicating that Nxph1-dependent effects of $GABA_BR$ may have a specific physiological role in the intra-NRT network. For example, there is a slower oscillatory frequency compared with VB cells (28), and focal corticothalamic excitatory inputs result in widespread inhibitory activity (28, 51).

To test the hypothesis from research on KO that Nxph1 supports presynaptic $GABA_BR$, we expressed Nxph1 ectopically at excitatory terminals in the neocortex, which normally do not contain this molecule (Fig. 4). Our results show that presynaptic $GABA_BR$ and postsynaptic $GABA_AR$ together cause the diminished facilitation at transgenic excitatory synapses because the phenotype could be reversed by pharmacologically blocking $GABA_BR$ with CGP-55845, and a complete rescue was achieved by additional blocking of postsynaptic $GABA_AR$ with intracellular picrotoxin or gabazine (Fig. 6*A*; Fig. 7*E*; Fig. 8; Fig. S3*B*). Because GABAR blockers are effective at transgenic excitatory synapses, we conclude that ambient GABA is available in these contacts, either by co-release with Glu or by spillover from neighbored GABAergic terminals (52, 53). We suggest that, during paired-pulse experiments at transgenic synapses, the depolarization caused by glutamate receptors is countered by the activation of postsynaptic $GABA_AR$ that may short-circuit the excitation, thus resulting in reduced facilitation. Postsynaptically caused modulation of long-term synaptic plasticity by $GABA_AR$ has been shown (54), and the presence of a low number of postsynaptic $GABA_AR$ at WT excitatory synapses may serve to regulate the time course of excitation and to limit glutamatergic overexcitation and subsequent excitotoxicity as summarized in ref. 41. Therefore, the recruitment of (additional) postsynaptic $GABA_AR$ triggered by our ectopic expression of Nxph1 may enhance a natural process and thus explain the alterations of short-term plasticity as observed in our study. Moreover, coactivation of presynaptic $GABA_BR$ at the transgenic excitatory synapses may curtail glutamate release itself, thus further decreasing the possiblity of facilitation (55). In fact, this regulatory action of presynaptic $GABA_BR$ is well-documented for many excitatory and inhibitory synapses (55–60), suggesting that recruitment of (additional) presynaptic $GABA_BR$ triggered by our ectopic expression of Nxph1 may again only enhance a natural process. Finally, in both mouse models and types of synapses investigated, evoked release (eIPSC in NRT and eEPSC in neocortex) was unchanged over a range of stimulation strengths, suggesting that the efficiency of

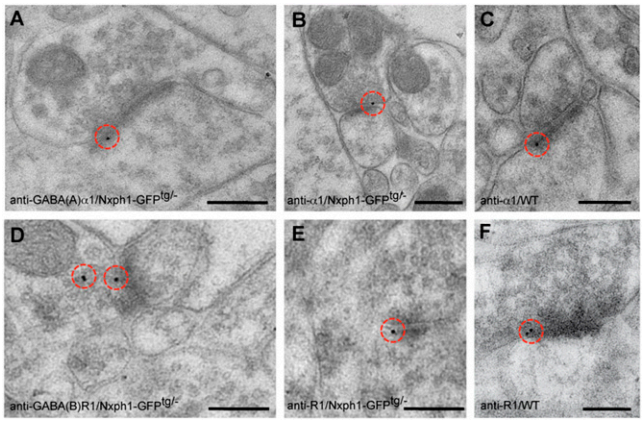

Fig. 8. Localization of $GABA_AR$ and $GABA_BR$ subunits at Nxph1-expressing excitatory synapses. (*A* and *B*) Immunogold labeling with anti-$GABA_AR\alpha1$ in Lowicryl-embedded Nxph1-GFP$^{tg/-}$ neocortex frequently demonstrates the presence of this subunit at asymmetric (presumptive excitatory) synapses compared with control animals (for quantification, see *Expression of Nxph1 Has an Instructive Role in Synapses*). (*C*) Asymmetric terminals in WT neocortex only rarely show labeling for $GABA_AR\alpha1$ subunits. (*D–F*) Similar experiment to *A–C* using antibodies against $GABA_BR1$ subunits. Immunoelectron microscopy demonstrates more abundant labeling of $GABA_BR$ at excitatory synapses in the cortex of Lowicryl-embedded Nxph1-GFP$^{tg/-}$ brains (*D* and *E*), but WT terminals (*F*) can also contain these subunits (for quantification, see *Expression of Nxph1 Has an Instructive Role in Synapses*). Red circles mark 10-nm gold particles. (Scale bars, 100 nm.)

basal transmission or probability of release is not prominently affected by the presence of Nxph1. Analysis of spontaneous release, in turn, gave uneven results in the two models: Although the increase in mini frequency in NRT neurons of Nxph1 KO (Fig. 1*C*) can be explained by impaired/missing $GABA_BR$ because blocking with CGP in WT neurons mimicked this effect (Fig. 2 *B* and *E*), consistent with published results (31), transgenic expression of Nxph1 did not affect the mini frequency in cortical excitatory synapses (Fig. 5*B*). Such differences of spontaneous release in response to alterations of presynaptic $GABA_BR$, however, are not very surprising as $GABA_BR$-mediated effects are highly dependent on the brain region and/or type of terminal (43, 61).

The role of Nxph1 in distinct inhibitory synapses of the NRT as uncovered here is in line with the high expression of Nxph1 in this thalamic nucleus (19) (and qRT-PCR data in this study). Moreover, the lack of a significant phenotype at GABAergic synapses in the VB and the neocortex reflects low expression of Nxph1 in interneurons of these regions (19) (and qRT-PCR data in this study). A compensatory role of other members of the Nxph family is not likely to play a role because Nxph2 is not expressed in rodent brains (22), Nxph3 expression is restricted to subpopulations of glutamatergic neurons (20), and Nxph4 does barely bind to α-Nrxn due to a long linker insertion between domains (23). Future experiments will also have to address the question if the other α-Nrxn–binding variant, Nxph3, is similarly used to tune synapse plasticity at excitatory terminals (20).

Nxph1 Alters the Molecular Composition of Synapses. Although our study shows that Nxph1 modulates the presence of $GABA_BR$ and $GABA_AR$, Nxph1 is not generally required for receptor function. For example, Nxph1 may contribute to the heterogeneity of $GABA_BR$ responses as demonstrated recently for KCTD proteins (62), possibly by stabilizing the receptors at a subpopulation of synapses. Similarly, the effect on $GABA_AR$ is also not ubiquitous because functional $GABA_AR\alpha1$ subunits with fast decay time constants (63) were found at Nxph1-expressing transgenic synapses, but changes of evoked $GABA_AR$-mediated currents were largely absent in KO NRT recordings. One possible explanation is that GABAergic transmission in the NRT relies mostly on the $GABA_AR\alpha3$ subunit (64–66), which may not be a target of Nxph1.

The involvement of $GABA_AR$ at transgenic synapses is a striking result because it raises the question if it is Nxph1 alone or the complex of Nxph1/α–Nrxn that is responsible for the phenotype. α-Nrxn itself, the only known binding partner for Nxph1 thus far (19, 22, 23), affects inhibitory synaptic function (7, 9, 37, 67) and even interacts directly with the $GABA_AR\alpha1$ subunit (37). The role of α-Nrxn in synaptic function has attracted attention because α-Nrxn are essential for neurotransmission and implicated in neuropsychiatric disorders (reviewed in refs. 5 and 6). Apart from Nxph, prototypical binding partners of Nrxn are neuroligins (13, 14), LRRTMs (15, 16), and cerebellin/GluRδ2 (17, 18). Physical binding has also been reported for $GABA_AR$ subunits (37); dystroglycan (68); and, very recently, calsyntenin-3 (67). In addition, research has identified several molecules, mostly ion channels and receptors, which are functionally impaired when Nrxn expression is altered. Nrxn variants have been found to affect voltage-dependent calcium channels (9, 10), $GABA_AR$ (7, 37), NMDAR (44), $GABA_BR$ (36, 45), nicotinergic acetylcholine receptors (69), and AMPAR (47). These ionotropic and metabotropic receptors represent "target molecules" of Nrxn that may include some physical association, but it appears unlikely that the functional link to all these requires stable protein–protein interactions. Thus, presence of Nxph1 in complex with α-Nrxn may modulate the spectrum of target molecules.

Presence of Nxph1 at presynaptic terminals of specific subpopulations of interneurons may also help to diversify the properties of inhibitory synapses. In contrast to the mostly splice-code–dependent *trans*-synaptic interactions of Nrxn (13, 14, 18, 68, 70, 71), binding of Nxph1 is splice-site independent (23) and has a high degree of local specificity due to its restricted expression in subpopulations of GABAergic interneurons (19). This is an important aspect because the preferred neuroligin variant of α-Nrxn at GABAergic contacts, neuroligin2 (7, 72), has been shown to similarly regulate defined subsets of inhibitory connections (73). It has been argued that α-Nrxn/neuroligin2 represent a strong candidate pair for specific inhibitory *trans*-synaptic interactions (8, 74–77), and our data on Nxph1 at inhibitory synapses strengthen this association. These data suggest that the presence of Nxph1 at synapses represents a previously unrecognized variable that modulates the activity of GABAR. It is important to note, however, that our results do not imply that $GABA_AR$ or $GABA_BR$ at inhibitory synapses are an exclusive target of Nxph1/α–Nrxn. In fact, we reported previously that the $GABA_BR$-mediated modulation of $Ca_V2.2$ channels, required for its effect on vesicle release (58), was also impaired at excitatory brainstem synapses of α-Nrxn KO mice (45). Even more importantly, α-Nrxn is abundantly expressed in glutamatergic neurons as well (12) and has unequivocal effects on release from excitatory synapses (9, 44, 46, 78). These results cannot be explained by a simple association of α-Nrxn with inhibitory and, of β-Nrxn with excitatory terminals as cautioned before (37). Although coexpression of Nxph1 could serve as a means to diversify the cellular functions of α-Nrxn at subpopulations of terminals, the mechanistic basis for this possibility remains to be elucidated.

Materials and Methods

Animals. Mice of wild-type, Nxph1-GFP transgenic, or Nxph1-deficient genotypes were used and experiments were approved by the Landesamt für Natur, Umwelt und Verbraucherschutz, North Rhine-Westphalia (license 84-02.05.20.11.209), and confirmed by the Institutional Animal Care and Use Committee of the Medical Faculty of the Westfälische Wilhelms-University, Münster, Germany. For details, see *SI Materials and Methods*.

RT-qPCR. For details, see *SI Materials and Methods*.

Electrophysiological Experiments. WT, Nxph1-GFP$^{tg/-}$, and Nxph1 KO mice [postnatal days 14–21(P14–P21)] were used for patch-clamp recordings. After anesthesia, brains were transferred into ice-cold artificial cerebrospinal fluid (ACSF) (in mM: 118 NaCl, 3 KCl, 1 NaH_2PO_4, 20 glucose, 1.5 $CaCl_2$, 1 $MgCl_2$,

25 $NaHCO_3$, pH 7.3, ~305 mOsmol), gassed with 95% (vol/vol) O_2 and 5% (vol/vol) CO_2. Frontal slices (300 μm) containing the somatosensory cortex (WT, Nxph1-GFP$^{tg/-}$, and Nxph1 KO) and slices containing the NRT of WT and Nxph1 KO were incubated at 35 °C in ACSF for 1 h before recordings. For NRT, the extracellular Ca^{2+} concentration was elevated to 3 mM to analyze low-threshold spikes.

Recording procedures. Whole-cell patch-clamp recordings in voltage-clamp and current-clamp mode were performed at 30 °C on layer 5 pyramidal cells (Nxph1-GFP$^{tg/-}$ and Nxph1 KO) and on GABAergic NRT neurons (Nxph1 KO mice), using a fixed-stage microscope (water immersion ×40 objective, differential interference contrast/infrared optics). Borosilicate glass pipettes had resistances between 2 and 4 MΩ and were filled with different internal solutions: (*i*) for electrically evoked excitatory and inhibitory postsynaptic currents (eEPSCs and eIPSCs) and excitatory miniature postsynaptic current (mEPSC) recordings (in mM): 140 K-gluconate, 1 $CaCl_2$, 10 Hepes, 2 $MgCl_2$, 4 Na-ATP, 0.5 Na-GTP, 10 EGTA, pH 7.3, 300 mOsmol, plus 5 mM lidocaine to prevent sodium spikes; (*ii*) for mIPSCs, K-gluconate was exchanged by KCl; and (*iii*) for current-clamp recordings (in mM): 90 K-gluconate, 20 K-citrate, 0.5 $CaCl_2$, 10 Hepes, 1 $MgCl_2$, 10 NaCl, 15 phosphocreatine, 3 Na-ATP, 0.5 Na-GTP, 3 K-BAPTA, pH 7.3, 295 mOsmol. For two-step tip-filling experiments (39), the initial 500 μm of the pipette was prefilled with solution without blocker and then the remainder of the pipette was backfilled with internal solution containing 200 μM picrotoxin or 50 μM gabazine. Electrical stimulations used a concentric bipolar electrode. Only neurons with membrane input resistances between 80 and 560 MΩ, resting membrane potentials between −55 and −80 mV, and input capacitance of 30–150 pF were selected for analysis. To analyze intrinsic properties of NRT neurons (LTS), cells were held near their resting potential at −60 to −70 mV, followed by eight steps of current injections, starting with −150 pA (increasing in 50-pA steps; 500-ms duration). The hyperpolarizing current injections evoked LTS bursts, and depolarizing current injections induced a series of action potentials.

Basal synaptic transmission. mPSCs were recorded in the presence of 500 nM tetrodotoxin in combination with 5 μM bicuculline for mEPSC at −70 mV or with 20 μM CNQX (6-Cyano-7-nitroquinoxaline-2,3-dione disodium hydrate) for mIPSC at −70 mV. CGP-55845 (20 μM) was applied to block $GABA_BR$. Only mPSCs 4× larger than background noise were selected for analysis, and 100 individual events were fitted from each cell. Inter-event intervals, amplitudes, charge, and rise and decay times were calculated. eEPSCs were recorded at −80 mV (+ 2 μM bicuculline) and eIPSCs at −20 mV [+ 25 μM APV (D-(-)-2-Amino-5-phosphonopentanoic acid) and 20 μM CNQX], using single 90-μs stimulation shocks given with increasing strengths (0.02–0.2 mA for neocortex, 0.1–0.5 mA for NRT) by a stimulation electrode in layer 5. Maximal PSCs and amplitudes at low and half-maximum stimulation intensities were recorded, and input/output relations, amplitudes, and time constants were calculated.

GABA-dependent PSCs. Local application of 10 mM GABA was delivered through pipettes filled with extracellular ACSF. The puff pipette was positioned in proximity to recorded cells with constant puff pressure (13 psi) and duration (500 ms). At least 10 sweeps were recorded at 50-s intervals, and GABA-dependent PSCs measured at −20 mV in the presence of 20 μM CNQX and 25 μM APV. CGP-55845 (20 μM) was added to the bathing solution to block $GABA_BR$ as indicated, and 20 μM bicuculline and 20 μM gabazine were applied to block $GABA_AR$ for verification of GABA-dependent PSCs at the end of each recording.

Synaptic short-term plasticity. PPR was calculated from recordings of ePSCs at half-maximal stimulation intensities for most conditions. Weaker stimulus intensities were used during blockade of GABAR. PPR was defined as the ratio of second to first amplitude of two consecutive ePSCs. Stimuli were applied 10× with 20-s breaks, and interstimulus intervals varied from 20 to 200 ms. In 20-Hz stimulus trains, consisting of 10 pulses, the ratios were defined as the 10th to the 1st, the 4th to the 1st, and the 2nd to the 1st amplitude. For pharmacological blocking, 200 μM picrotoxin or 50 μM gabazine was added to the pipette solution to block $GABA_AR$ intracellularly (79–83), and PPR was measured immediately or after 10 min, as indicated. Bicuculline (2 μM) and/or 20 μM CGP-55845 was added to the bathing solution to block $GABA_AR$ and $GABA_BR$.

Data acquisition and statistical analysis. Acquisition and analysis used EPC-10 USB amplifiers and software Patchmaster, Fitmaster, MiniAnalysis, and Microsoft Excel. Statistical significance was tested with a two-tailed unpaired Student *t* test using GraphPad Prism software. Exact *P* values and numbers of recorded cells per genotype are given in *Results* or figure legends.

Electron Microscopy. Brain tissue from WT and Nxph1-GFP$^{tg/-}$ mice was embedded in epon resin or Lowicryl HM20 using freeze substitution in methanol. For cryosectioning, anesthetized mice were transcardially perfused with 70 mL of 0.2% glutaraldehyde (GA) and 2% paraformaldehyde, postfixed at 4 °C, and slices were infiltrated with 2.3 M sucrose at 4 °C. Tissue blocks were frozen in liquid N_2, and ribbons of cryosections were cut at −100 °C and transferred with 2.3 M sucrose/2% methyl cellulose to Formvar-coated gold or carbon-coated copper grids.

Immunogold labeling. Ultrathin Epon sections were placed on droplets of blocking solution (0.15% glycine/PBS) for 2 h, followed by 20% normal goat serum (NGS) for 20 min, incubated with rabbit–anti-GFP in 10% NGS/PBS for 30 min and with 10 nm gold-conjugated secondary goat–anti-rabbit antibody for 30 min. Staining of Lowicryl sections started with blocking on 2% human serum albumin/0.05 M tris-buffered saline droplets. Incubation with anti-GFP, $GABA_AR\alpha1$, or $GABA_BR1$ followed overnight at 4 °C, and 10 nm gold antibody for 2 h at room temperature (RT). For cryosections, blocking with 0.05 M glycine/PBS and 0.1% BSA for 15 min/step was followed by anti-GFP incubation in 0.1% BSA/PBS at RT for 3 h and 10 nm gold antibody for 2 h at RT. Labeled sections were postfixed with 1% GA and contrasted with neutral uranylacetate.

Ultrastructural analysis. Immunogold-labeled synapses were documented with a Libra 120 TEM (80 kV; 2,048 × 2,048 CCD; ITEM software). For synapse morphometry, image series including all cortical layers on 17 multiple image alignment (MIA) pictures were examined (each MIA = 100 μm^2). Asymmetric (type 1) and symmetric (type 2) synapses were quantified as area densities, and randomly chosen synapses were analyzed for presynaptic terminal area, number of vesicles per terminal area, postsynaptic-density length, and synaptic cleft width. Statistical significance was evaluated with GraphPad Prism, and exact *P* values and number of samples/repeats are given in *Results* or figure legends.

ACKNOWLEDGMENTS. We thank G. Szabo (KOKI) for the kind gift of GAD65_GFP mice, K. Kerkhoff and D. Aschhoff for excellent technical assistance, K. Piechotta for help with molecular cloning during early stages of the project, and members of our laboratories for discussion. This work was supported by Deutsche Forschungsgemeinschaft Grant SFB 629-TPB11 (to M.M.) and Grant SFB/TRR58-TPA03 (to H.-C.P.), Cells-in-Motion Cluster of Excellence (EXC 1003 to M.M., H.-C.P., and F.K.), and the Interdisziplinäres Zentrum für Klinische Forschung Münster Mi 3/025/08 (to M.M.). S.W. is recipient of a fellowship by the Graduate School Cell Dynamics and Disease.

1. Rozov A, Burnashev N, Sakmann B, Neher E (2001) Transmitter release modulation by intracellular Ca2+ buffers in facilitating and depressing nerve terminals of pyramidal cells in layer 2/3 of the rat neocortex indicates a target cell-specific difference in presynaptic calcium dynamics. *J Physiol* 531(Pt 3):807–826.
2. Abbott LF, Regehr WG (2004) Synaptic computation. *Nature* 431(7010):796–803.
3. Branco T, Staras K, Darcy KJ, Goda Y (2008) Local dendritic activity sets release probability at hippocampal synapses. *Neuron* 59(3):475–485.
4. Südhof TC, Rothman JE (2009) Membrane fusion: Grappling with SNARE and SM proteins. *Science* 323(5913):474–477.
5. Südhof TC (2008) Neuroligins and neurexins link synaptic function to cognitive disease. *Nature* 455(7215):903–911.
6. Reissner C, Runkel F, Missler M (2013) Neurexins. *Genome Biol* 14(9):213.
7. Graf ER, Zhang X, Jin SX, Linhoff MW, Craig AM (2004) Neurexins induce differentiation of GABA and glutamate postsynaptic specializations via neuroligins. *Cell* 119(7):1013–1026.
8. Chih B, Engelman H, Scheiffele P (2005) Control of excitatory and inhibitory synapse formation by neuroligins. *Science* 307(5713):1324–1328.
9. Missler M, et al. (2003) Alpha-neurexins couple Ca2+ channels to synaptic vesicle exocytosis. *Nature* 423(6943):939–948.
10. Zhang W, et al. (2005) Extracellular domains of alpha-neurexins participate in regulating synaptic transmission by selectively affecting N- and P/Q-type Ca2+ channels. *J Neurosci* 25(17):4330–4342.
11. Ushkaryov YA, Petrenko AG, Geppert M, Südhof TC (1992) Neurexins: Synaptic cell surface proteins related to the alpha-latrotoxin receptor and laminin. *Science* 257(5066):50–56.
12. Ullrich B, Ushkaryov YA, Südhof TC (1995) Cartography of neurexins: More than 1000 isoforms generated by alternative splicing and expressed in distinct subsets of neurons. *Neuron* 14(3):497–507.
13. Boucard AA, Chubykin AA, Comoletti D, Taylor P, Südhof TC (2005) A splice code for trans-synaptic cell adhesion mediated by binding of neuroligin 1 to alpha- and beta-neurexins. *Neuron* 48(2):229–236.
14. Ichtchenko K, et al. (1995) Neuroligin 1: A splice site-specific ligand for beta-neurexins. *Cell* 81(3):435–443.
15. de Wit J, et al. (2009) LRRTM2 interacts with Neurexin1 and regulates excitatory synapse formation. *Neuron* 64(6):799–806.
16. Ko J, Fuccillo MV, Malenka RC, Südhof TC (2009) LRRTM2 functions as a neurexin ligand in promoting excitatory synapse formation. *Neuron* 64(6):791–798.
17. Matsuda K, et al. (2010) Cbln1 is a ligand for an orphan glutamate receptor delta2, a bidirectional synapse organizer. *Science* 328(5976):363–368.
18. Uemura T, et al. (2010) Trans-synaptic interaction of GluRdelta2 and Neurexin through Cbln1 mediates synapse formation in the cerebellum. *Cell* 141(6):1068–1079.
19. Petrenko AG, et al. (1996) Structure and evolution of neurexophilin. *J Neurosci* 16(14):4360–4369.

20. Beglopoulos V, et al. (2005) Neurexophilin 3 is highly localized in cortical and cerebellar regions and is functionally important for sensorimotor gating and motor coordination. *Mol Cell Biol* 25(16):7278–7288.
21. Petrenko AG, et al. (1993) Polypeptide composition of the alpha-latrotoxin receptor. High affinity binding protein consists of a family of related high molecular weight polypeptides complexed to a low molecular weight protein. *J Biol Chem* 268(3): 1860–1867.
22. Missler M, Südhof TC (1998) Neurexophilins form a conserved family of neuropeptide-like glycoproteins. *J Neurosci* 18(10):3630–3638.
23. Missler M, Hammer RE, Südhof TC (1998) Neurexophilin binding to alpha-neurexins. A single LNS domain functions as an independently folding ligand-binding unit. *J Biol Chem* 273(52):34716–34723.
24. Batista-Brito R, Machold R, Klein C, Fishell G (2008) Gene expression in cortical interneuron precursors is prescient of their mature function. *Cereb Cortex* 18(10): 2306–2317.
25. Guillery RW, Harting JK (2003) Structure and connections of the thalamic reticular nucleus: Advancing views over half a century. *J Comp Neurol* 463(4):360–371.
26. Fuentealba P, Steriade M (2005) The reticular nucleus revisited: Intrinsic and network properties of a thalamic pacemaker. *Prog Neurobiol* 75(2):125–141.
27. Pinault D (2004) The thalamic reticular nucleus: Structure, function and concept. *Brain Res Brain Res Rev* 46(1):1–31.
28. Ulrich D, Huguenard JR (1996) Gamma-aminobutyric acid type B receptor-dependent burst-firing in thalamic neurons: A dynamic clamp study. *Proc Natl Acad Sci USA* 93(23):13245–13249.
29. Bal T, McCormick DA (1993) Mechanisms of oscillatory activity in guinea-pig nucleus reticularis thalami in vitro: A mammalian pacemaker. *J Physiol* 468:669–691.
30. Coulon P, et al. (2009) Burst discharges in neurons of the thalamic reticular nucleus are shaped by calcium-induced calcium release. *Cell Calcium* 46(5–6):333–346.
31. Ulrich D, Huguenard JR (1996) GABAB receptor-mediated responses in GABAergic projection neurones of rat nucleus reticularis thalami in vitro. *J Physiol* 493(Pt 3): 845–854.
32. Davies CH, Collingridge GL (1993) The physiological regulation of synaptic inhibition by GABAB autoreceptors in rat hippocampus. *J Physiol* 472:245–265.
33. Isaacson JS, Solís JM, Nicoll RA (1993) Local and diffuse synaptic actions of GABA in the hippocampus. *Neuron* 10(2):165–175.
34. Zucker RS, Regehr WG (2002) Short-term synaptic plasticity. *Annu Rev Physiol* 64: 355–405.
35. Kraushaar U, Jonas P (2000) Efficacy and stability of quantal GABA release at a hippocampal interneuron-principal neuron synapse. *J Neurosci* 20(15):5594–5607.
36. Fu Y, Huang ZJ (2010) Differential dynamics and activity-dependent regulation of alpha- and beta-neurexins at developing GABAergic synapses. *Proc Natl Acad Sci USA* 107(52):22699–22704.
37. Zhang C, et al. (2010) Neurexins physically and functionally interact with GABA(A) receptors. *Neuron* 66(3):403–416.
38. Johnston GA (2013) Advantages of an antagonist: Bicuculline and other GABA antagonists. *Br J Pharmacol* 169(2):328–336.
39. Rae J, Cooper K, Gates P, Watsky M (1991) Low access resistance perforated patch recordings using amphotericin B. *J Neurosci Methods* 37(1):15–26.
40. Ruiz A, Campanac E, Scott RS, Rusakov DA, Kullmann DM (2010) Presynaptic GABAA receptors enhance transmission and LTP induction at hippocampal mossy fiber synapses. *Nat Neurosci* 13(4):431–438.
41. Shrivastava AN, Triller A, Sieghart W (2011) GABA(A) receptors: Post-synaptic co-localization and cross-talk with other receptors. *Front Cell Neurosci* 5:7.
42. Fritschy JM, et al. (1999) GABAB-receptor splice variants GB1a and GB1b in rat brain: Developmental regulation, cellular distribution and extrasynaptic localization. *Eur J Neurosci* 11(3):761–768.
43. Chalifoux JR, Carter AG (2011) GABAB receptor modulation of synaptic function. *Curr Opin Neurobiol* 21(2):339–344.
44. Kattenstroth G, Tantalaki E, Südhof TC, Gottmann K, Missler M (2004) Postsynaptic N-methyl-D-aspartate receptor function requires alpha-neurexins. *Proc Natl Acad Sci USA* 101(8):2607–2612.
45. Dudanova I, et al. (2006) Important contribution of alpha-neurexins to Ca2+-triggered exocytosis of secretory granules. *J Neurosci* 26(41):10599–10613.
46. Etherton MR, Blaiss CA, Powell CM, Südhof TC (2009) Mouse neurexin-1alpha deletion causes correlated electrophysiological and behavioral changes consistent with cognitive impairments. *Proc Natl Acad Sci USA* 106(42):17998–18003.
47. Aoto J, Martinelli DC, Malenka RC, Tabuchi K, Südhof TC (2013) Presynaptic neurexin-3 alternative splicing trans-synaptically controls postsynaptic AMPA receptor trafficking. *Cell* 154(1):75–88.
48. Kwon HB, Sabatini BL (2011) Glutamate induces de novo growth of functional spines in developing cortex. *Nature* 474(7349):100–104.
49. Dobie FA, Craig AM (2011) Inhibitory synapse dynamics: Coordinated presynaptic and postsynaptic mobility and the major contribution of recycled vesicles to new synapse formation. *J Neurosci* 31(29):10481–10493.
50. Chen JL, et al. (2012) Clustered dynamics of inhibitory synapses and dendritic spines in the adult neocortex. *Neuron* 74(2):361–373.
51. Zhang L, Jones EG (2004) Corticothalamic inhibition in the thalamic reticular nucleus. *J Neurophysiol* 91(2):759–766.
52. Hnasko TS, Edwards RH (2012) Neurotransmitter corelease: Mechanism and physiological role. *Annu Rev Physiol* 74:225–243.
53. Rusakov DA, Savtchenko LP, Zheng K, Henley JM (2011) Shaping the synaptic signal: Molecular mobility inside and outside the cleft. *Trends Neurosci* 34(7):359–369.
54. Shen H, et al. (2010) A critical role for alpha4betadelta GABAA receptors in shaping learning deficits at puberty in mice. *Science* 327(5972):1515–1518.
55. Porter JT, Nieves D (2004) Presynaptic GABAB receptors modulate thalamic excitation of inhibitory and excitatory neurons in the mouse barrel cortex. *J Neurophysiol* 92(5): 2762–2770.
56. Pan BX, et al. (2009) Selective gating of glutamatergic inputs to excitatory neurons of amygdala by presynaptic GABAb receptor. *Neuron* 61(6):917–929.
57. Pérez-Garci E, Gassmann M, Bettler B, Larkum ME (2006) The GABAB1b isoform mediates long-lasting inhibition of dendritic Ca2+ spikes in layer 5 somatosensory pyramidal neurons. *Neuron* 50(4):603–616.
58. Laviv T, et al. (2011) Compartmentalization of the GABAB receptor signaling complex is required for presynaptic inhibition at hippocampal synapses. *J Neurosci* 31(35): 12523–12532.
59. Poncer JC, McKinney RA, Gahwiler BH, Thompson SM (2000) Differential control of GABA release at synapses from distinct interneurons in rat hippocampus. *J Physiol* 528(Pt 1):123–130.
60. Fu Y, Wu X, Lu J, Huang ZJ (2012) Presynaptic GABA(B) receptor regulates activity-dependent maturation and patterning of inhibitory synapses through dynamic allocation of synaptic vesicles. *Front Cell Neurosci* 6:57.
61. Otis TS, Mody I (1992) Differential activation of GABAA and GABAB receptors by spontaneously released transmitter. *J Neurophysiol* 67(1):227–235.
62. Schwenk J, et al. (2010) Native GABA(B) receptors are heteromultimers with a family of auxiliary subunits. *Nature* 465(7295):231–235.
63. Eyre MD, Renzi M, Farrant M, Nusser Z (2012) Setting the time course of inhibitory synaptic currents by mixing multiple GABA(A) receptor α subunit isoforms. *J Neurosci* 32(17):5853–5867.
64. Mozrzymas JW, Barberis A, Vicini S (2007) GABAergic currents in RT and VB thalamic nuclei follow kinetic pattern of alpha3- and alpha1-subunit-containing GABAA receptors. *Eur J Neurosci* 26(3):657–665.
65. Schofield CM, Kleiman-Weiner M, Rudolph U, Huguenard JR (2009) A gain in GABAA receptor synaptic strength in thalamus reduces oscillatory activity and absence seizures. *Proc Natl Acad Sci USA* 106(18):7630–7635.
66. Fritschy JM, Mohler H (1995) GABAA-receptor heterogeneity in the adult rat brain: Differential regional and cellular distribution of seven major subunits. *J Comp Neurol* 359(1):154–194.
67. Pettem KL, et al. (2013) The specific α-neurexin interactor calsyntenin-3 promotes excitatory and inhibitory synapse development. *Neuron* 80(1):113–128.
68. Sugita S, et al. (2001) A stoichiometric complex of neurexins and dystroglycan in brain. *J Cell Biol* 154(2):435–445.
69. Cheng SB, et al. (2009) Presynaptic targeting of alpha4beta 2 nicotinic acetylcholine receptors is regulated by neurexin-1beta. *J Biol Chem* 284(35):23251–23259.
70. Iijima T, et al. (2011) SAM68 regulates neuronal activity-dependent alternative splicing of neurexin-1. *Cell* 147(7):1601–1614.
71. Siddiqui TJ, Pancaroglu R, Kang Y, Rooyakkers A, Craig AM (2010) LRRTMs and neuroligins bind neurexins with a differential code to cooperate in glutamate synapse development. *J Neurosci* 30(22):7495–7506.
72. Varoqueaux F, Jamain S, Brose N (2004) Neuroligin 2 is exclusively localized to inhibitory synapses. *Eur J Cell Biol* 83(9):449–456.
73. Gibson JR, Huber KM, Südhof TC (2009) Neuroligin-2 deletion selectively decreases inhibitory synaptic transmission originating from fast-spiking but not from somatostatin-positive interneurons. *J Neurosci* 29(44):13883–13897.
74. Chubykin AA, et al. (2007) Activity-dependent validation of excitatory versus inhibitory synapses by neuroligin-1 versus neuroligin-2. *Neuron* 54(6):919–931.
75. Kang Y, Zhang X, Dobie F, Wu H, Craig AM (2008) Induction of GABAergic postsynaptic differentiation by alpha-neurexins. *J Biol Chem* 283(4):2323–2334.
76. Poulopoulos A, et al. (2009) Neuroligin 2 drives postsynaptic assembly at perisomatic inhibitory synapses through gephyrin and collybistin. *Neuron* 63(5):628–642.
77. Futai K, Doty CD, Baek B, Ryu J, Sheng M (2013) Specific trans-synaptic interaction with inhibitory interneuronal neurexin underlies differential ability of neuroligins to induce functional inhibitory synapses. *J Neurosci* 33(8):3612–3623.
78. Sons MS, et al. (2006) alpha-Neurexins are required for efficient transmitter release and synaptic homeostasis at the mouse neuromuscular junction. *Neuroscience* 138(2):433–446.
79. Inomata N, Tokutomi N, Oyama Y, Akaike N (1988) Intracellular picrotoxin blocks pentobarbital-gated Cl- conductance. *Neurosci Res* 6(1):72–75.
80. Nelson S, Toth L, Sheth B, Sur M (1994) Orientation selectivity of cortical neurons during intracellular blockade of inhibition. *Science* 265(5173):774–777.
81. Mancilla JG, Ulinski PS (2001) Role of GABA(A)-mediated inhibition in controlling the responses of regular spiking cells in turtle visual cortex. *Vis Neurosci* 18(1):9–24.
82. Metherate R, Ashe JH (1993) Ionic flux contributions to neocortical slow waves and nucleus basalis-mediated activation: Whole-cell recordings in vivo. *J Neurosci* 13(12): 5312–5323.
83. Blundon JA, Bayazitov IT, Zakharenko SS (2011) Presynaptic gating of postsynaptically expressed plasticity at mature thalamocortical synapses. *J Neurosci* 31(44):16012–16025.